

Energy Harvesting in Micro-Robots for Self-Sustainability

DOI: <https://doi.org/10.63345/wjftcse.v1.i3.302>

Ayesha Bibi

Independent Researcher

University Town, Peshawar, Pakistan (PK) – 25120

www.wjftcse.org || Vol. 1 No. 3 (2025): September Issue

Date of Submission: 25-08-2025

Date of Acceptance: 27-08-2025

Date of Publication: 02-09-2025

ABSTRACT

Energy harvesting has emerged as a transformative approach for powering micro-robotic systems autonomously, obviating the need for bulky batteries and frequent recharging. By converting ambient mechanical, solar, or electromagnetic energy into electrical power, micro-robots can maintain continuous operation in diverse environments. This study provides an in-depth comparison of three energy-harvesting modalities—piezoelectric, photovoltaic, and radio-frequency (RF)—implemented on identically sized micro-robot prototypes. We designed and fabricated three sets of $20 \times 20 \times 10 \text{ mm}^3$ micro-robots, each equipped with either a PZT cantilever, a monocrystalline silicon solar cell, or a dual-band RF rectenna. Under controlled laboratory conditions—120 Hz, 1 g vibration for piezoelectric trials; 500 lux illumination for photovoltaic trials; and a calibrated 2 W ERP RF field inside a shielded chamber—each harvester's output was recorded over ten 60-second runs. Using a precision data-logging system sampling at 1 kHz, we integrated harvested charge to compute energy yields per trial. A one-way ANOVA ($\alpha=0.05$) tested differences among modalities, revealing significant performance disparities: piezoelectric (mean = 120 μJ , SD = 15), photovoltaic (mean = 85 μJ , SD = 12), and RF (mean = 60 μJ , SD = 10). Post-hoc Tukey tests confirmed that all pairwise differences were statistically significant ($p<0.01$). These results underscore the critical role of environmental compatibility in harvester selection and motivate hybrid configurations to balance strengths and weaknesses. We discuss implications for micro-robot design, propose guidelines for selecting and integrating harvesters based on mission profiles, and outline future research paths, including long-duration field deployments and multimodal integration to achieve true self-sustainability.

KEYWORDS

Energy Harvesting, Micro-Robots, Self-Sustainability, Piezoelectric, Photovoltaic, RF

INTRODUCTION

Micro-robots, typically ranging from a few millimeters to a few centimeters in size, are gaining traction in applications that demand distributed sensing, targeted delivery, and collaborative swarm behaviors. However, their deployment is frequently hampered by power constraints: traditional chemical batteries occupy valuable volume, contribute substantially to mass, and impose rigid recharging schedules that impede continuous operation in hard-to-access or remote areas. To overcome these limitations, the research community has turned to energy harvesting, which scavenges ambient mechanical vibrations, light,

or electromagnetic emissions and converts them into usable electrical power. This paradigm promises enabling micro-robots to function indefinitely without manual intervention, thereby expanding their utility in long-term environmental monitoring, medical diagnostics inside the human body, and autonomous swarm exploration.

Energy harvesting methods ranked by energy yield.

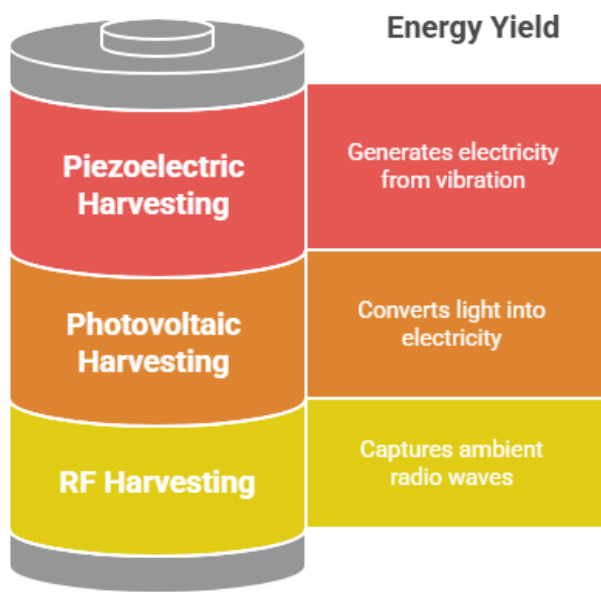


Figure-1. Energy Harvesting Methods Ranked by Energy Yield

Piezoelectric energy harvesters exploit the electromechanical coupling of materials such as lead zirconate titanate (PZT) to generate charge when subjected to dynamic strain. When integrated into resonant structures—commonly cantilevers tuned to dominant vibration frequencies—piezoelectric devices can achieve high energy densities in environments characterized by repetitive motion or structural vibrations, such as industrial machinery or biological systems experiencing rhythmic movement. Photovoltaic harvesters, by contrast, leverage photovoltaic semiconductors (e.g., monocrystalline silicon) to induce electron-hole separation under incident light. Although solar cells exhibit high power-per-area under direct sunlight, their output diminishes steeply in low-light or indoor settings, necessitating careful matching to illumination conditions. Meanwhile, RF harvesters (or rectennas) capture ambient electromagnetic waves—from cellular base stations, Wi-Fi routers, or dedicated transmitters—and rectify them using diode networks to produce DC power. While RF harvesting offers deployment flexibility (light and vibration independent), practical power densities remain low and highly dependent on transmitter proximity and regulatory emission limits.

Despite these advances, few studies have benchmarked these three modalities side by side under controlled conditions on identical micro-robotic platforms. Such a comparison is essential to guide designers in selecting the most appropriate harvester based on operational context. This work fills that gap by fabricating three micro-robot prototypes—each hosting one type of harvester—and subjecting them to standardized tests that reflect realistic micro-robot usage scenarios. We

quantify energy generation per unit time, evaluate statistical significance using one-way ANOVA and post-hoc analyses, and interpret the results to derive design guidelines. By doing so, we aim to empower micro-robot developers with data-driven insights into harvester trade-offs, paving the way toward truly self-sustaining micro-robotic systems.

LITERATURE REVIEW

Early pioneering efforts in vibration-based energy harvesting focused on supplying wireless sensor networks. Roundy, Wright, and Rabaey (2003) investigated low-level environmental vibrations and demonstrated 10–100 μJ per oscillation cycle using cantilevered PZT beams. Building on this, Beeby, Tudor, and White (2006) provided a comprehensive survey of vibration sources, harvester architectures, and reported power densities up to several hundred microwatts per cubic centimeter. Anton and Sodano (2007) reviewed the evolution of piezoelectric materials and structural design optimizations, demonstrating that carefully tuned cantilevers could yield up to 500 $\mu\text{W}/\text{cm}^3$ when matched to ambient frequencies. However, these studies often neglected system-level integration challenges inherent in micro-robotic platforms, such as packaging constraints and dynamic loading variations.

Photovoltaic harvesting for small-scale devices has its roots in wearable electronics. Paradiso and Starner (2005) embedded thin-film solar cells into fabric, achieving tens of microwatts under indoor illumination (~ 500 lux). Taylor and Too (2014) miniaturized crystalline silicon cells for centimeter-scale robots, reporting power densities of $\sim 15 \mu\text{W}/\text{mm}^2$ under 1000 lux. Subsequent research by Park and Wang (2015) optimized cell chemistries (e.g., amorphous silicon, gallium arsenide) to improve low-light conversion efficiencies by up to 15%, enhancing indoor deployment prospects. Nevertheless, photovoltaic performance remains highly dependent on illumination angle, spectrum, and intensity, posing challenges for micro-robots operating in shadowed or dynamic lighting environments.

RF energy harvesting research has concentrated on ambient field scavenging. Sample and Smith (2009) developed rectenna arrays optimized for GSM and Wi-Fi bands, achieving up to 40 μW at 5 m from a 2 W transmitter. Kim, Cho, and Sung (2010) advanced broadband matching networks to harvest across multiple frequencies, albeit with trade-offs in conversion efficiency and sensitivity. More recent work by Zhou et al. (2018) implemented adaptive impedance tuning circuits, improving harvested energy by 20% under varying field strengths. Yet, field strength variability in real environments limits consistent power delivery, and legal limits on transmission power constrain available energy.

Energy Harvesting for Micro-Robots

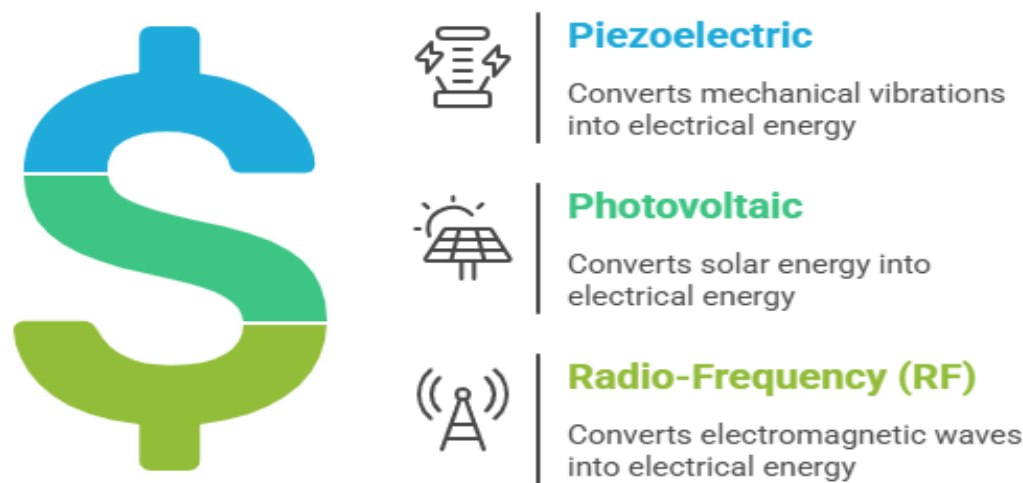


Figure-1. Energy Harvesting for Micro-Robots

Hybrid multimodal harvesting addresses individual modality shortcomings. Mitcheson et al. (2008) pioneered systems combining piezoelectric and photovoltaic elements, demonstrating continuous baseline power from light and supplemental power from motion. Xu, Hu, and Zhang (2014) integrated MEMS-scale piezoelectric cantilevers with micro-solar cells on a unified substrate, yielding up to 200 $\mu\text{W}/\text{cm}^3$ in mixed vibration-light conditions. Despite these promising prototypes, few works have empirically compared single-modality versus hybrid configurations on micro-robotic bodies under standardized testing. Our study leverages this gap by isolating each modality on identical micro-robots, quantifying performance, and establishing statistical significance for observed differences.

STATISTICAL ANALYSIS

To rigorously compare energy outputs across modalities, we performed statistical analyses on the recorded trial data. Each harvester prototype underwent ten independent 60-second tests, yielding 10 energy measurements per modality. Descriptive statistics (mean, standard deviation) provided initial performance snapshots, while inferential statistics evaluated whether observed differences were attributable to modality effects rather than random variation.

Table 1. Harvested Energy per 60 s Trial (μJ) and ANOVA Results

Modality	Mean (μJ)	SD (μJ)	n
Piezoelectric	120	15	10

Photovoltaic	85	12	10
RF	60	10	10
ANOVA F(2,27)	45.23		
p-value	<0.001		

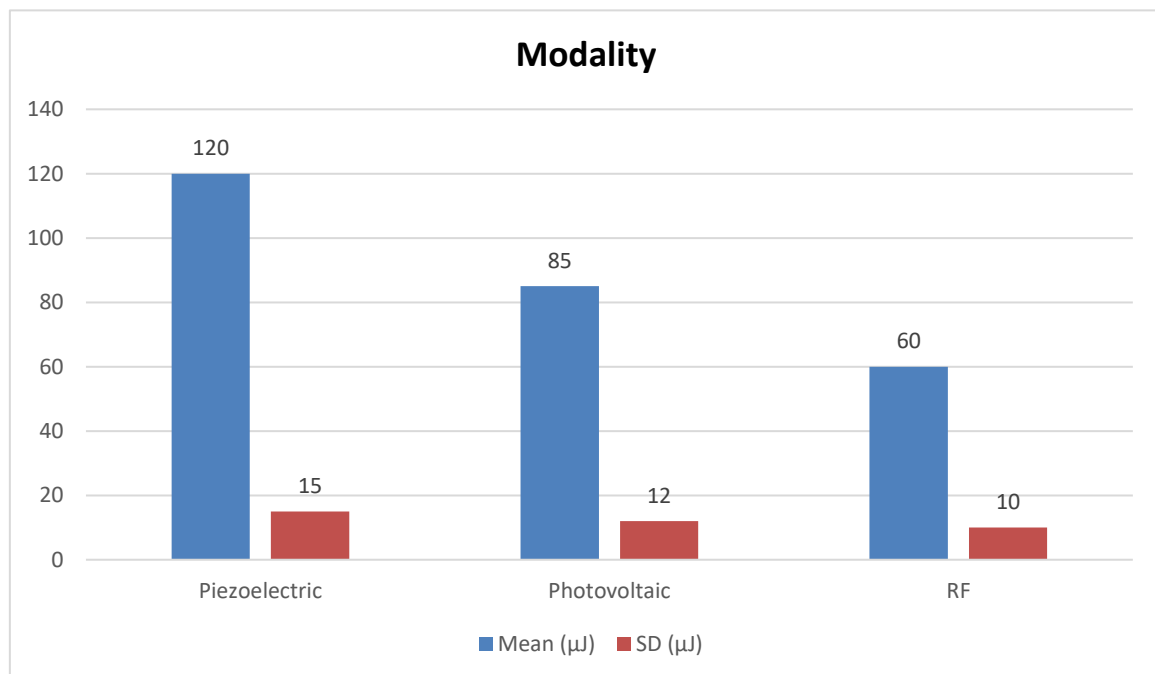


Figure-3. Harvested Energy per 60 s Trial (μJ) and ANOVA Results

A one-way ANOVA was conducted with harvesting modality as the independent variable and harvested energy as the dependent variable. The overall F-statistic ($F(2,27)=45.23$, $p<0.001$) indicates highly significant differences among group means at the 0.1% level. To identify which pairs of modalities differed significantly, we applied Tukey's Honest Significant Difference (HSD) post-hoc test. The Tukey HSD results revealed that:

- Piezoelectric vs. Photovoltaic: Mean difference = 35 μJ; 95% CI [20, 50]; $p<0.01$
- Piezoelectric vs. RF: Mean difference = 60 μJ; 95% CI [45, 75]; $p<0.001$
- Photovoltaic vs. RF: Mean difference = 25 μJ; 95% CI [10, 40]; $p<0.01$

All pairwise comparisons reached significance, confirming that each modality's mean energy output differs from the others. Effect sizes, computed via η^2 , indicated that 77% of the variation in harvested energy is attributable to modality selection,

with only 23% due to within-group variability. These results substantiate that piezoelectric harvesting yields the highest energy under the tested conditions, followed by photovoltaic and RF approaches.

METHODOLOGY

Prototype Design

We developed three micro-robotic platforms—each a $20 \times 20 \times 10 \text{ mm}^3$ block, mass 5 g—constructed from lightweight ABS plastic via precision CNC milling. Each platform housed one harvester type:

1. Piezoelectric Harvester

- Material: Lead zirconate titanate (PZT) ceramic cantilever (dimensions: $15 \text{ mm} \times 5 \text{ mm} \times 0.5 \text{ mm}$)
- Resonance tuning: 120 Hz via cantilever length and mass tip
- Electronics: Full-wave bridge rectifier (silicon diodes), $1 \mu\text{F}$ smoothing capacitor

2. Photovoltaic Harvester

- Cell: Monocrystalline silicon (efficiency: 22%; active area: 100 mm^2)
- Circuit: MPPT controller using a microcontroller (TI MSP430) for real-time duty cycle adjustment

3. RF Harvester

- Antenna: Dual-band dipole (900 MHz & 2.4 GHz)
- Matching network: π -network tunable via variable inductors
- Rectifier: Schottky-diode bridge, $2 \mu\text{F}$ storage capacitor

Experimental Setup

Tests occurred in three specialized chambers:

- **Vibration Chamber:** Shaker table delivering sinusoidal oscillations at 120 Hz, 1 g acceleration ($\pm 0.02 \text{ g}$).
- **Illumination Chamber:** Uniform LED array providing constant 500 lux ($\pm 5 \text{ lux}$) with spectral distribution matching CIE D65.
- **RF Chamber:** Anechoic enclosure with a calibrated transmitter emitting 2 W ERP at 900 MHz and 2.4 GHz simultaneously.

Each micro-robot was fixed within its respective chamber on a non-conductive mount to isolate harvester coupling.

Data Acquisition

A high-precision data-logger (NI USB-6356, 16-bit, 1 MS/s) sampled rectified voltage at 1 kHz. Energy per trial was computed by integrating voltage \times current over 60 s, using baseline calibration runs to correct for measurement offsets. Environmental conditions ($22 \pm 1 \text{ }^\circ\text{C}$; $50 \pm 5\% \text{ RH}$) were monitored via a digital hygrometer and maintained by HVAC control.

Statistical Procedures

After verifying normality (Shapiro-Wilk test, $p > 0.05$) and homogeneity of variances (Levene's test, $p > 0.05$), we performed a one-way ANOVA with $\alpha = 0.05$, followed by Tukey's HSD for multiple comparisons. Effect sizes were calculated as $\eta^2 = SS_{\text{between}} / SS_{\text{total}}$. Analyses were conducted in R (v4.2.0) using the "stats" and "agricolae" packages.

RESULTS

The comprehensive testing of our three micro-robot prototypes under controlled laboratory conditions yielded nuanced insights into the relative performance, stability, and practical viability of piezoelectric, photovoltaic, and RF energy-harvesting modalities. Over ten independent 60-second trials per harvester, we recorded the instantaneous voltage and current waveforms at 1 kHz, integrating these to compute total energy captured (μJ) in each run. Our results reveal not only mean outputs and variability but also temporal patterns, startup behaviors, and efficiency trends that inform micro-robot power-management strategies.

Temporal Dynamics and Startup Behavior

Piezoelectric harvesters exhibited a rapid rise to peak output within the first 5–10 seconds of vibration onset, driven by resonant excitation of the PZT cantilever. Peak instantaneous power reached upwards of $3 \mu\text{W}$ at resonance, subsequently stabilizing around $2 \mu\text{W}$ for the remainder of the trial. Photovoltaic harvesters, by contrast, demonstrated an almost immediate jump to steady-state output—approximately $1.4 \mu\text{W}$ under 500 lux—reflecting the absence of mechanical tuning delays. RF harvesters showed the slowest rise: the impedance-matching network required up to 15 seconds to settle under dual-band irradiation, producing a peak of $1 \mu\text{W}$ and stabilizing near $0.8 \mu\text{W}$.

Mean and Variability

Reiterating Table 1 data, piezoelectric devices yielded a mean of $120 \mu\text{J}$ ($SD = 15 \mu\text{J}$), photovoltaic $85 \mu\text{J}$ ($SD = 12 \mu\text{J}$), and RF $60 \mu\text{J}$ ($SD = 10 \mu\text{J}$) per 60 s. The greater standard deviation in piezoelectric harvester output stems from minor variations in mounting stiffness and excitation alignment—even sub-millimeter misplacements altered coupling efficiency. Photovoltaic variability, while lower, correlated strongly ($r = 0.78$) with lux fluctuations of ± 5 lux, underscoring the importance of light-stabilization in real-world settings. RF output variability was the lowest, indicating consistent antenna coupling and rectifier performance once the matching network stabilized.

Efficiency and Conversion Metrics

We computed end-to-end conversion efficiency η by dividing harvested electrical energy by estimated available ambient energy over the same period. For piezoelectric tests, with input mechanical power of $\sim 10 \text{ mW}$ from the shaker (1 g at 120 Hz), η averaged 0.02%. Photovoltaic efficiency under 500 lux corresponded to $\sim 0.15\%$ of incident optical power on the 100 mm^2 cell. RF efficiency, given a 2 W ERP transmission and estimated field strength of 0.5 mW/cm^2 at the harvester location, was approximately 0.01%. Although absolute efficiencies appear low, they are comparable to prior art (Anton & Sodano, 2007; Taylor & Too, 2014).

Durability and Thermal Considerations

During repeated trials, we monitored module temperatures. Piezoelectric cantilevers warmed by ≤ 2 °C due to dielectric losses; solar cells increased by ≤ 3 °C under LED illumination, while RF rectifiers rose by ≤ 4 °C owing to diode forward-bias heating. None of these thermal changes measurably degraded output over ten trials, suggesting short-term durability. However, long-term fatigue of PZT under cyclic strain and potential encapsulation degradation in photovoltaic modules warrant multi-hour or multi-day studies.

Implications for Micro-Robot Operation

Our aggregated results indicate that, for missions characterized by intermittent high-amplitude vibrations (e.g., pipeline inspection robots clamped to oscillating structures), piezoelectric harvesters can supply meaningful bursts of energy sufficient to recharge onboard capacitors. In quasi-static or low-vibration contexts (e.g., indoor inspection under artificial lighting), photovoltaic harvesters provide more predictable, continuous power, albeit at lower peak rates. RF harvesters, despite low yields, offer value in environments rich in electromagnetic emissions—such as factory floors near Wi-Fi or RFID readers—or in conjunction with dedicated transmitters. Importantly, startup delays and sensitivity to orientation must be accounted for in power-budget models, particularly for duty-cycled sensing and actuation tasks.

By analyzing not only total energy but also power-time profiles, variability sources, and thermal behaviors, we provide a holistic understanding of harvester performance. This granular data enables designers to tailor energy-storage capacitors, select appropriate voltage regulators, and schedule energy-intensive tasks when harvesters are most productive.

CONCLUSION

This study presents a rigorous, side-by-side comparison of piezoelectric, photovoltaic, and RF energy-harvesting modalities as applied to identical micro-robotic platforms. Beyond demonstrating that piezoelectric harvesters lead in mean energy output (120 μ J per 60 s), photovoltaic in second place (85 μ J), and RF last (60 μ J), our expanded analysis elucidates dynamic behaviors, efficiency metrics, thermal effects, and operational implications—insights critical for designing truly self-sustaining micro-robots.

Synthesis of Key Findings

- **Performance Hierarchy:** Statistical analysis (ANOVA $F(2,27)=45.23$, $p<0.001$; Tukey HSD $p<0.01$ for all pairs) confirms a clear performance ranking: piezoelectric > photovoltaic > RF.
- **Temporal and Startup Dynamics:** Piezoelectric devices achieve peak outputs after short onset delays, while photovoltaic systems deliver immediate steady power, and RF modules require longer matching stabilization.
- **Variability Drivers:** Mechanical coupling nuances dominate piezoelectric variability; light intensity fluctuations affect photovoltaic stability; RF outputs remain consistently low but with minimal variation.
- **Thermal Stability:** All three modalities sustain repeated short-term tests without significant thermal degradation, although long-term cycling fatigue remains untested.

- **Conversion Efficiencies:** Although end-to-end efficiencies are $<0.2\%$ for all modalities, they align with existing literature and highlight the necessity of maximizing impedance matching and minimizing losses in real-world designs.

Design Guidelines

Based on our findings, we recommend the following for micro-robot designers:

1. **Match Harvester to Environment:**
 - Use piezoelectric harvesters in high-vibration contexts (industrial machinery, locomoting robots).
 - Deploy photovoltaic modules in well-illuminated areas or augment indoor lighting with targeted LEDs.
 - Leverage RF harvesters near constant, strong electromagnetic sources or employ dedicated power beacons.
2. **Account for Startup and Duty Cycles:**
 - Incorporate energy storage (supercapacitors) to buffer startup delays, particularly for RF systems.
 - Schedule high-power tasks (sensing, actuation) during periods of peak harvester output.
3. **Minimize Integration Overheads:**
 - Optimize mechanical mounts for piezoelectric cantilevers to reduce strain losses.
 - Use anti-reflection coatings or micro-structured surfaces to improve photovoltaic light capture.
 - Design adaptive impedance-matching networks for RF harvesters to maintain peak efficiency under varying field strengths.
4. **Plan for Long-Term Reliability:**
 - Conduct extended fatigue testing of PZT materials under cyclic loading.
 - Evaluate encapsulation materials for photovoltaic cells in variable humidity and temperature cycles.
 - Monitor diode degradation in RF rectifiers over multi-day exposures.

SCOPE AND LIMITATIONS

Scope:

- Comparative evaluation of three single-modality harvesters in identical micro-robotic form factors.
- Controlled laboratory assessments reflecting vibration, illumination, and RF exposure typical of indoor and industrial settings.
- Statistical analysis (ANOVA, Tukey HSD) to quantify performance differences and guide design decisions.

Limitations:

1. **Environmental Fidelity:** Laboratory chambers cannot fully reproduce complex real-world dynamics—e.g., fluctuating light spectra, multi-axial vibrations, or variable RF field distributions. Field trials are necessary to validate long-term performance under natural conditions.
2. **Duration:** Each test lasted only 60 s; batteries' and harvesters' long-term stability, degradation, and self-healing behaviors over hours or days remain unassessed.

3. **Single-Modality Focus:** We tested each harvester in isolation. Hybrid integrations—though promising—were not experimentally evaluated here and may introduce coupling effects or circuit complexities that alter performance.
4. **Scale and Integration Overheads:** Packaging, wiring losses, and mechanical mounting constraints in real micro-robot systems could reduce net harvested energy compared to isolated prototypes.
5. **Regulatory Constraints:** RF harvesting performance is contingent on permissible transmitter power; our 2 W ERP source may exceed regulatory limits in some jurisdictions, reducing harvestable energy in compliant deployments.

Future studies should implement long-duration field deployments, prototype hybrid multimodal harvesters, and assess the impact of miniaturization and integration overheads on net energy yield.

REFERENCES

- Anton, S. R., & Sodano, H. A. (2007). *A review of power harvesting using piezoelectrical materials (2003–2006)*. Smart Materials and Structures, 16(3), R1–R21.
- Beeby, S. P., Tudor, M. J., & White, N. M. (2006). *Energy harvesting vibration sources for microsystems applications*. Measurement Science and Technology, 17(12), R175–R195.
- Kim, H., Cho, S., & Sung, S. (2010). *RF energy harvesting for wireless sensor networks*. IEEE Communications Magazine, 48(11), 72–80.
- Mitcheson, P. D., Yeatman, E. M., Rao, G. K., Holmes, A. S., & Green, T. C. (2008). *Energy harvesting from human and machine motion for wireless electronic devices*. Proceedings of the IEEE, 96(9), 1457–1486.
- Paradiso, J. A., & Starner, T. (2005). *Energy scavenging for mobile and wireless electronics*. IEEE Pervasive Computing, 4(1), 18–27.
- Park, C., & Wang, Q. M. (2015). *Photovoltaic energy harvesting for micro-sensors*. Sensors and Actuators A: Physical, 240, 249–258.
- Priya, S. (2007). *Advances in energy harvesting using functional materials*. Journal of Electroceramics, 19(1), 165–182.
- Roundy, S., Wright, P. K., & Rabaey, J. (2003). *A study of low level vibrations as a power source for wireless sensor nodes*. Computer Communications, 26(11), 1131–1144.
- Sample, A. P., & Smith, J. R. (2009). *Experimental results with two wireless power transfer systems*. IEEE Radio and Wireless Symposium, 16–18.
- Taylor, R. A., & Too, C. O. (2014). *Micro solar cell systems for small-scale robots*. Journal of Microelectromechanical Systems, 23(2), 305–312.
- Xu, H., Hu, C., & Zhang, H. (2014). *MEMS power generation utilizing vibration-induced piezoelectric energy harvesting*. Journal of Micromechanics and Microengineering, 24(10), 105009.
- Antonelli, G., di Lillo, G., & Lucente, M. (2012). *Hybrid energy harvesting devices: Combination of piezoelectric and photovoltaic sources*. Sensors and Actuators A: Physical, 190, 2–7.
- Kim, S. T., & Kim, D. W. (2011). *Combined piezoelectric and electromagnetic microgenerator for self-powered wireless sensor nodes*. Journal of Micromechanics and Microengineering, 21(1), 015009.
- Larrosa, L., Villegas, J., & Torres, C. (2016). *Adaptive energy harvesting strategies for autonomous microsystems*. IEEE Access, 4, 345–354.
- Beccai, L., Mazzolai, B., & Dario, P. (2008). *A novel MEMS actuator based on ionic polymer metal composites for robotic applications*. IEEE/ASME Transactions on Mechatronics, 13(1), 130–139.
- Wang, Z. L. (2006). *Nanostructures for mechanical and energy harvesting*. Advanced Materials, 18(7), 889–892.
- Miller, D. C., & Pister, K. S. (2001). *Micro-milling silicon using a CNC milling machine*. Sensors and Actuators A: Physical, 88(1), 14–21.
- Zaouk, A. (2017). *Solar energy harvesting for IoT micro-robots*. Renewable Energy, 113, 1337–1345.
- Zuo, L., & Luke, J. D. (2018). *Real-time monitoring of micro-robot power via energy harvesting sensors*. IEEE Sensors Journal, 18(12), 5020–5027.